A Review of Charging Algorithms for Nickel and Lithium Battery Chargers

Ala Al-Haj Hussein, *Student Member, IEEE*, and Issa Batarseh, *Fellow, IEEE*

***Abstract*—Battery-charging algorithms can be used for either single- or multiple-battery chemistries. In general, single-chemistry chargers have the advantages of simplicity and reliability. On the other hand, multichemistry chargers, or "universal battery chargers," provide a practical option for multichemistry battery systems, particularly for portable appliances, but they have some limitations. This paper presents a review of some charging algorithms for major batteries, i.e., nickel–cadmium, nickel–metal–hydride, and lithium-ion batteries for single- and multiple-chemistry chargers. A comparison between these algorithms in terms of their charging schemes and charge termination techniques is included. In addition, some trends of recent chargers development are presented.**

***Index Terms*—Constant current (CC), constant voltage (CV), inflection point, open-circuit voltage (OCV), pulse charging, state of charge (SOC), trickle charging, voltage drop.**

I. Introduction

RECHARGEABLE batteries were first introduced in 1859 when the first rechargeable lead–acid battery was invented by the French inventor Gaston Plante [1]. Lead–acid batteries are used in several applications where cost is more important than space and weight, typically preferred as backup batteries for uninterruptable power supply (UPS) and alarm systems, as well as automotive lighting and ignition applications (unsuitable for portable appliances). Almost four decades beyond this invention, the nickel–cadmium (NiCd) battery was invented and widely used in low-power applications. One major limitation of NiCd batteries is the "memory effect" phenomenon, which is a term used to describe the degradation in the battery capacity when it is partly charged and discharged. In addition, because of cadmium, these batteries are not environmentally friendly. Then, in the 1990s, nickel–metal–hydride (NiMH) and lithium-ion (Li-ion) batteries were invented and commercialized. These batteries have higher energy and power densities compared with lead–acid and NiCd batteries and do not suffer from the memory effect. In particular, Li-ion batteries have the highest energy/power density, life-cycles, as well as the highest cost.

Manuscript received November 1, 2009; revised October 26, 2010; accepted December 13, 2010. Date of publication January 17, 2011; date of current version March 21, 2011. This work was supported in part by the National Science Foundation and by the Florida Energy Systems Consortium. The review of this paper was coordinated by Dr. C. C. Mi.

The authors are with the Department of Electrical Engineering and Computer Science, University of Central Florida, Orlando, FL 32816 USA (e-mail: aalhajhu@mail.ucf.edu; batarseh@mail.ucf.edu).

Color versions of one or more of the figures in this paper are available online at http://ieeexplore.ieee.org.

Digital Object Identifier 10.1109/TVT.2011.2106527

According to [2], battery charging is the most substantial issue in battery management systems. Basically, a charger has the following three functions: 1) delivering charge to the battery; 2) optimizing the charge rate; and 3) terminating the charge. The charge can be delivered to the battery through different charging schemes, depending on the battery chemistry. For example, nickel batteries require only constant current (CC), whereas Li-ion batteries require constant current/constant voltage (CC/CV). The charge rate can be optimized if the capacity and state of charge (SOC) are given. As an example, a completely discharged or a fully charged battery must be trickle charged with a very low current (a fraction of the capacity rate) to extend the battery life when it is completely discharged and to sustain the full charge in the battery when it is fully charged. In addition to CC and CC/CV charging schemes, pulse charging, which uses a pulse current for up to 1 s, followed by a rest period and a discharge pulse for milliseconds, is claimed to be optimal, because it improves the charging speed and efficiency [3]. With regard to the charge termination, different techniques are used, such as the voltage drop and temperature rise in nickel batteries or the inflection point (the point at which the sign of the second derivative of the voltage–time curve changes or the point at which the first derivative of the voltage–time curve is zero) in both nickel and lithium batteries. As a result of the diversity in battery systems and their applications, charging algorithms are, accordingly, also found to be diverse. For example, some algorithms are suitable for solar chargers [6], [12]. Other algorithms are suitable for single-chemistry chargers [4]–[10], whereas other algorithms are suitable for multichemistry chargers [12]–[14].

The scope of this paper is to compare and evaluate some charging algorithms for nickel and lithium batteries (lead–acid batteries are escaped due to the nature of their applications, which is different from nickel and lithium batteries). This paper compares the capabilities of these algorithms in optimizing the charging process in single-chemistry [4]–[10] and multichemistry [12]–[14] battery chargers. In this paper, Sections II and III present some recent single- and multiple-chemistry battery-charging algorithms, respectively. Section IV evaluates the discussed charging algorithms through real test data. Section V shows some trends of battery chargers. Finally, conclusions are drawn in Section VI.

II. Single-Chemistry Algorithms

Single-chemistry chargers are very common and are used in most battery systems. In this section, some charging algorithms for single-battery chemistries are discussed.

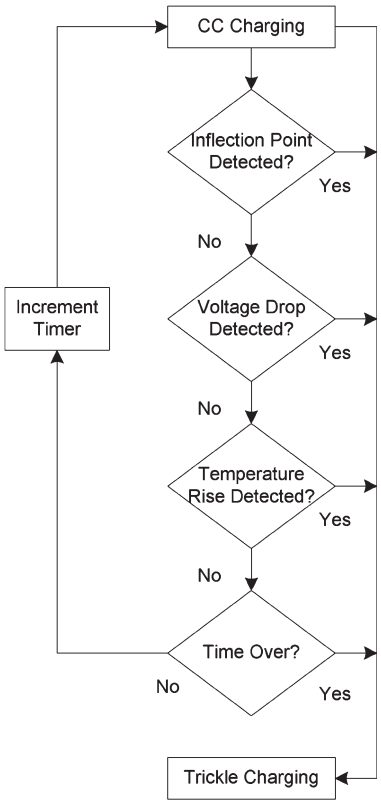

Fig. 1. Algorithm proposed in [4].

A. NiCd/NiMH Batteries

Because NiCd and NiMH single cells have the same cutoff voltages and the two battery types share almost the same performance during charging, they can be charged with the same charger. However, the charge termination method might be different for these batteries, which will be discussed later.

In [4], a NiCd/NiMH charging algorithm is proposed (see Fig. 1). A CC is used during charging until an inflection point is detected. Once an inflection point is detected, the charger switches to trickle charging to prevent overcharging the battery. Other charge termination techniques are implemented in this algorithm, e.g., voltage drop, temperature rise, and timing, to improve the charger performance.

Another charging algorithm is proposed in [5], which offers three charging stages. The algorithm is constructed from multiple statements. First, the voltage across the battery is sensed, and based on its value, an action is taken. For NiCd and NiMH battery packs, the voltage of each individual cell is found to be between 0.2 V and 1.6 V; otherwise, the battery is over (dis)charged. Within this range, the battery is charged with a relatively high current (fast charging) or low current (trickle charging) based on its voltage and temperature. When the battery voltage approaches 1.6 V, a trickle current is applied to the battery until it is removed from the charger.

Another algorithm is proposed in [6] for solar NiCd/NiMH battery chargers (see Fig. 2). The algorithm continuously tracks the maximum battery voltage and calculates the derivative of the voltage and the variation in the current in a sliding window of 5–10 min. The maximum voltage and the voltage drop will reset if at least the variation in the current or the derivative of the

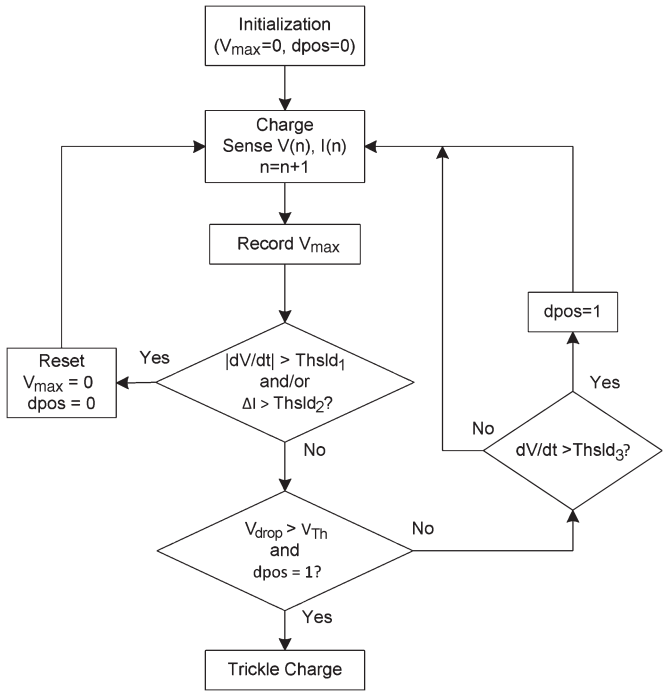

Fig. 2. "Voltage-based" algorithm proposed in [6].

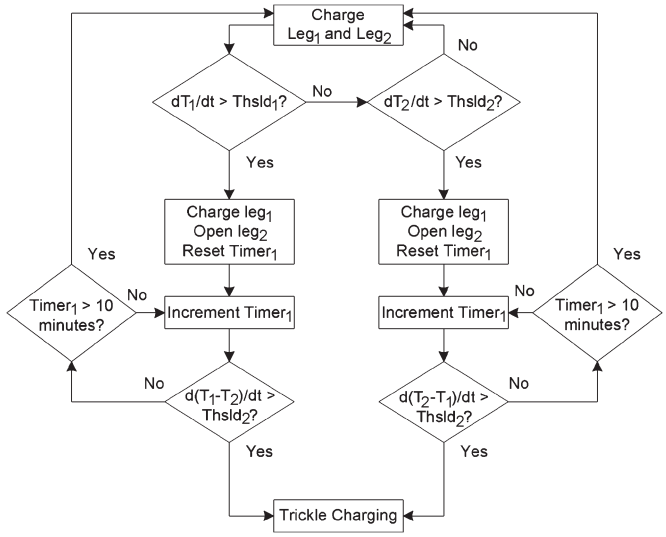

Fig. 3. "Temperature-based" algorithm proposed in [6].

voltage exceeds some predefined threshold values. Otherwise, the charging continues until a significant voltage rise (dV/dt > Thsld3), followed by a voltage drop above a certain threshold, occurs.

In the same work in [6], another algorithm is proposed (see Fig. 3). The concept of this algorithm is to divide the battery into two legs inside the battery pack and individually monitor the temperature of each leg. Ideally, the difference in temperature between the two legs must be negligible during charging, regardless of whether the ambient temperature changed. If a high positive temperature derivative is detected in one of the legs, the charger will keep charging this leg, whereas it stops charging the other leg. After a certain time, if the temperature derivative reaches a predefined threshold, then the algorithm will detect overcharge in that leg.

Another NiCd/NiMH charging algorithm is given in [7], in which the capacity of the battery must be provided. Charging starts by sensing the initial open-circuit voltage (OCV) to determine the battery SOC. In the first case, where the OCV is below 1 V/cell, the charger will inject a current of 0.1 C (C represents the capacity of the battery in ampere-hours) to charge the battery for 5 min. After the injection of the 5-min 0.1-C current, if the battery voltage was below 1.25 V/cell, this battery will be interpreted as damaged, and the charging will end. If the voltage was more than 1.25 V/cell after the 5-min 0.1-C current injection, a fast charging current will charge the battery until it becomes fully charged. In the second case, if the OCV was more than 1 V/cell, then, depending on this value, the battery will be in one of the following three states: 1) fully charged; 2) half charged; or 3) discharged. If the battery was discharged, it will initially be trickle charged to avoid damaging it with a high current. If the battery was half charged, it will initially be discharged and then charged to protect the battery from memory effect.

A different algorithm is proposed in [8], which utilizes the pulse-charging technique to charge NiCd and NiMH batteries. First, the battery initial OCV is sensed to determine the SOC of the battery. Based on the measured OCV, the battery is defined as one of the following three states: 1) fully charged (SOC $>$ 80%); 2) half charged (10% $\leq$ SOC $\leq$ 80%); or 3) discharged (SOC $<$ 10%). The charger measures the battery voltage, current, and temperature during charging. This method can support NiCd and NiMH of (0.6-, 0.9-, 1.2-, and 2-Ah) capacities as reported and requires the user to provide the battery capacity to the charger. If the temperature exceeded a certain range three times, charging will be halted, and the battery is considered damaged.

B. Li-Ion Batteries

Li-ion batteries have very critical charging requirements that must be met during charging to ensure preventing overheating and overcharging these batteries. Li-ion batteries are charged with a CV with a current limiter to prevent overheating in the initial stage of the charging. One special requirement for Li-ion chargers is to monitor the voltage across each cell when more than one cell is in a string (connected in series) to ensure charge balance and voltage equalization of the cells [16]. A protection circuit is usually added to the charger circuit to handle these functions.

A Li-ion battery-charging algorithm is proposed in [9] (see Fig. 4). In this algorithm, the temperature is constantly monitored during charging. Charging starts by measuring the initial OCV of the battery. If the value was between 2.9 V/cell and 4.2 V/cell, charging with a current of 0.7 C will hold until the upper voltage limit or a timeout is reached. Then, the CV mode starts until either the current drops below a threshold value or a timeout is reached. If the initial OCV was below 2.9 V/cell, charging with a current that is as low as 0.1 C will sustain until the OCV reaches 3 V/cell, at which fast charging current of 0.7 C will be applied. If the temperature during charging deviates from a certain range, the battery will be disconnected until its temperature return to the defined range. The charging will automatically be terminated after 720 min for safety.

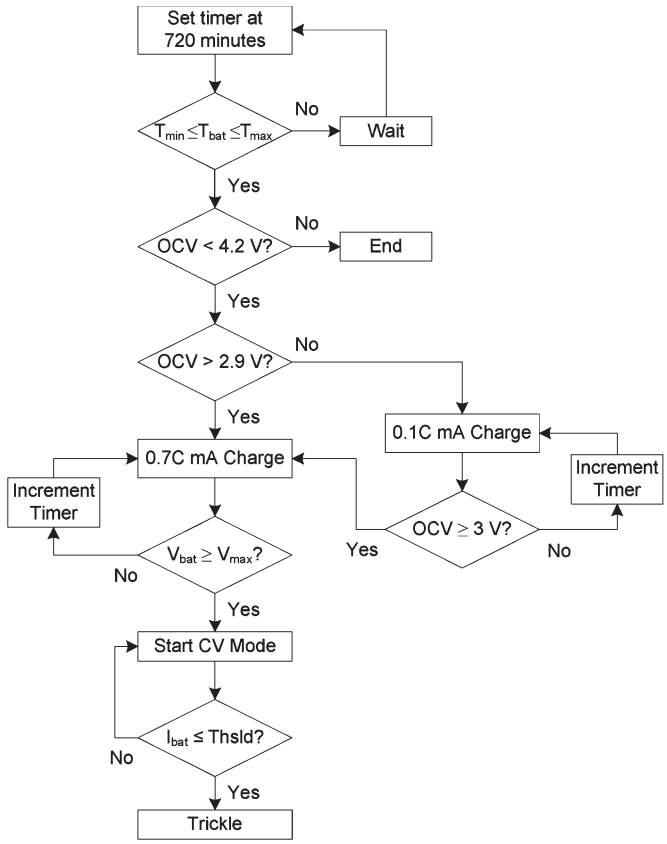

Fig. 4. Algorithm proposed in [9].

A similar algorithm is proposed in [10]. First, the OCV of the battery pack is sensed to check whether the battery is fully charged. If the battery is not fully charged, then the OCV of each individual cell is measured to check if the cells are unbalanced. The algorithm detects the unbalanced cells and fixes them before charging starts by discharging the overcharged cells until the difference in voltage between the highest and the lowest cell voltages return to an acceptable value below 0.1 V. Charging with CC will start when all cells' voltages are balanced and the temperature is in a predefined range until the upper safety voltage limit is reached. Then, the CV mode will start until the current drops to a threshold value at which charging will be terminated. In this algorithm, the battery module must be provided. During charging, if the voltage or temperature escaped the normal range, charging will be interrupted, and this condition will be interpreted as an error.

III. Multichemistry Algorithms

Due to the wide variety of portable appliances, ranging from toys and pocket lights to cell phones and personal digital assistants (PDAs), several chargers that can accommodate these enormous differences in applications have recently been developed. In multichemistry chargers, the main challenge is to detect the battery type and size to select the charging scheme and cutoffs. Therefore, these chargers require some techniques implemented in the controller to identify the battery and to ensure reliability and safety during charging. The discussion in this section includes some algorithms for nickel and lithium

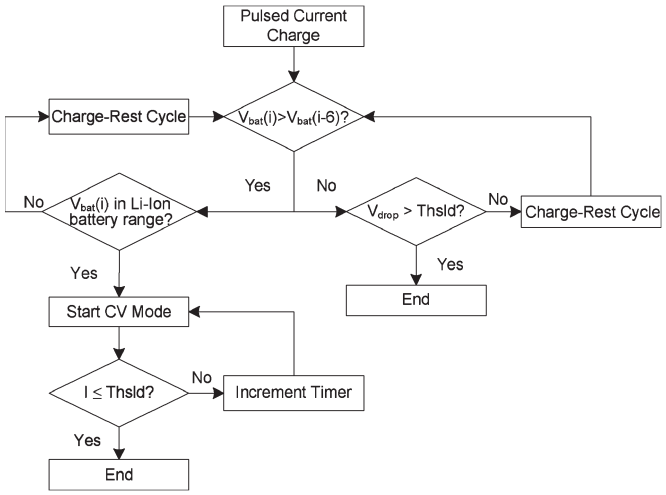

Fig. 5. Algorithm proposed in [12].

batteries. Although these algorithms can charge lead–acid batteries as reported, these batteries will be excluded from the discussion, because this paper focuses only on nickel and lithium batteries.

In [12], a solar battery charger algorithm is proposed to charge different batteries (see Fig. 5). The concept of interrupted charge control (ICC) used in [11] for standby applications was employed in [12] for bulk charging. The battery is charged with current pulses at a duty cycle of 50% to increase the accuracy of the voltage measurement at the end of each rest cycle. As reported, the charger speed can be improved when two batteries are simultaneously charged, because all the solar power is utilized to charge each battery in its charge cycle. The charger charges the battery with the current that was obtained from the solar array for 3 min (charge cycle) and disconnects the battery for another 3 min (rest cycle). The voltage at the end of each rest cycle is monitored and compared with the previous value. If the voltage increases, the algorithm checks if the voltage is within a predefined Li-ion range. If the voltage is not in one of the predefined ranges, charging will continue. The voltage drop is also monitored at the end of each rest cycle. If a voltage drop that is greater than a threshold value is detected, charging will be terminated, and the battery will be either a NiCd or a NiMH battery. If no voltage drop was detected and the battery voltage at the end of a rest cycle was in the safety limit range of Li-ion battery, the CV mode will start, and the current will be monitored until it drops below a threshold value at which charging will be terminated, and the battery will be Li-ion.

In [13], another multichemistry charging algorithm is proposed. A lookup table of OCVs of different possibilities of battery cells was established. First, the charger senses the OCV of the battery and compares it with the values in the lookup table. A possible safety limit voltage of a Li-ion battery is set to prevent damage in case of a Li-ion battery. Once the safety limit voltage is set, CC charging starts. During the CC mode, the "hysteresis measurement" test is performed to detect the battery chemistry. In this test, a discharge pulse of 2-A is applied to the battery for 30 s, and then, the battery is recharged with a 2-A pulse for another 30 s. If the difference in the

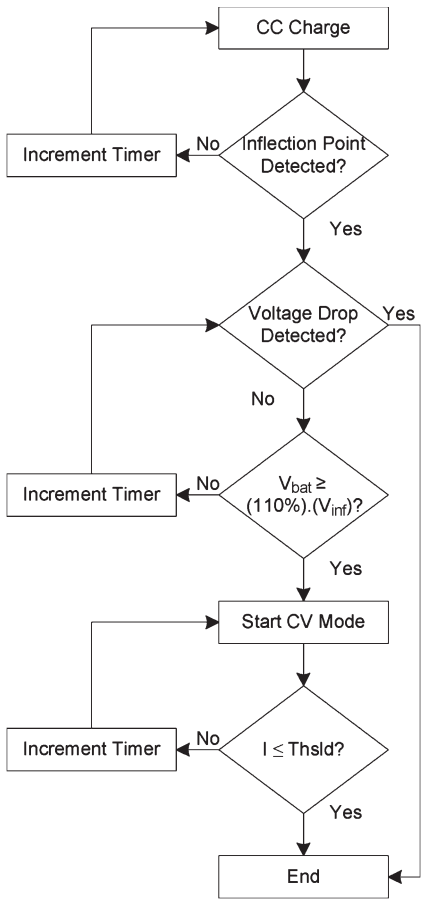

Fig. 6. Algorithm proposed in [14].

OCV of the battery after the discharge pulse and the charge pulse was greater than a minimum threshold, then the battery will be either NiCd or NiMH. Therefore, if a nickel battery was detected, charging with a CC will proceed until a voltage drop occurs, at which charging is terminated. If the battery chemistry was not detected from the hysteresis test, the charger will assume a Li-ion battery, and the CC mode will hold until the battery voltage reaches a predefined safety limit. If a voltage drop occurred before the safety limit is reached, charging will be terminated (a NiCd or a NiMH battery); otherwise, the CV mode will start and hold until the current drops below a threshold value.

Another multichemistry algorithm that uses the concept of the inflection point to identify the battery chemistry is proposed in [14] (see Fig. 6). In this algorithm, the battery is charged with a CC. The battery voltage and its first derivative are recorded at each time step. As reported in this paper, for NiCd and NiMH batteries, the peak voltage before the voltage drops is 6%–7% above the inflection point, whereas for Li-ion batteries, the upper voltage limit is around 10% above the inflection point. Based on this concept, the algorithm was designed to charge with a CC until either a voltage drop is detected (at about 6%–7% above the inflection point) or the voltage goes 10% above the inflection point, with no voltage drop detected, at which the CV mode starts until a predefined current drop is reached.

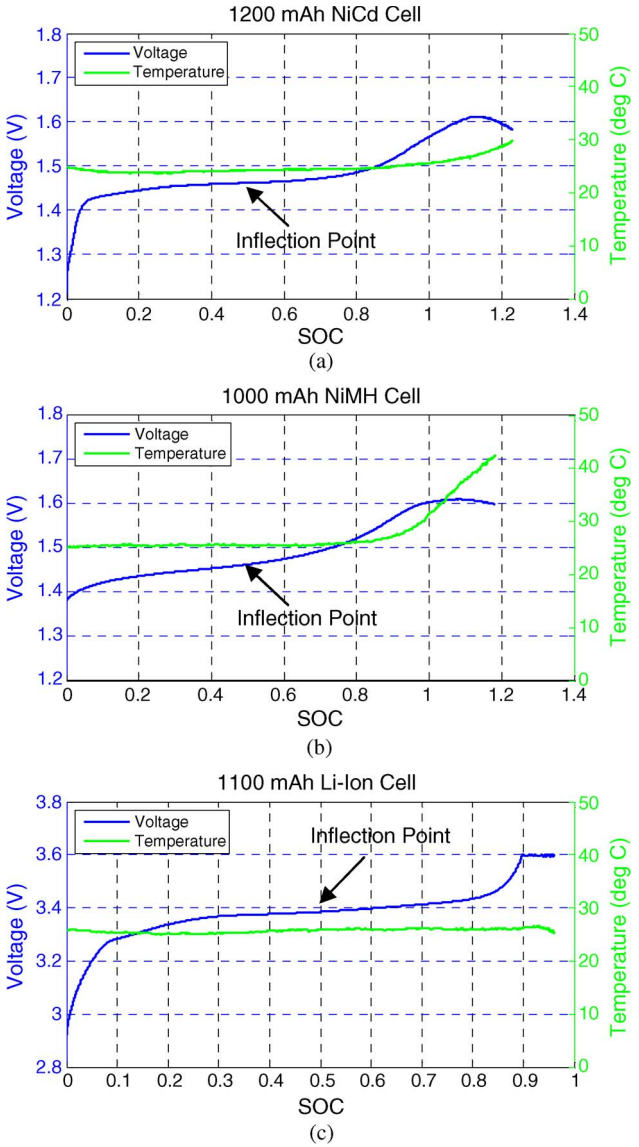

Fig. 7. Voltage and temperature profiles for charging (a) NiCd, (b) NiMH, and (c) Li-ion cells.

IV. Discussion on Reviewed Algorithms

The discussed charging algorithms incorporate simple techniques for managing the charging process, which may result in a possible overcharge or incomplete charge. This section discusses the capabilities of the reviewed algorithms through some test results. To compare and evaluate the discussed algorithms, some charging tests were performed on commercial NiCd, NiMH, and Li-ion single cells with capacities of 1200, 1000, and 1100 mAh, respectively. The cells were completely discharged and then completely charged. Fig. 7 shows the results, followed by a discussion (the horizontal axis represents the SOC, rather than time, for an in-depth evaluation).

A. Charging Process

In the reviewed algorithms, different control and measurement techniques were used during charging. The following discussion compares these techniques and points out their advantages and limitations.

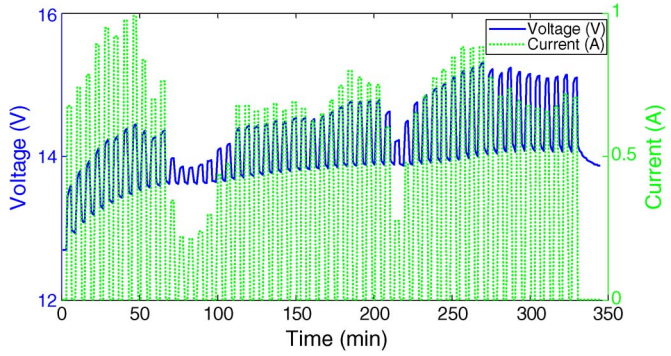

Fig. 8. ICC charging method in [12].

1) Charging Method: The charging methods employed in the discussed algorithms are mainly trickle, CC, and CC/CV. Trickle charging uses a very low current of a magnitude around 0.1 C to precharge a completely discharged battery (see [5] and [7]–[9]) or to sustain the charge in a fully charged battery (see [4] and [6]–[10]). A discharged battery is normally trickle charged for a short time to extend its life. On the other hand, CC and CC/CV are usually used for bulk charging. NiCd and NiMH batteries require only CC, whereas Li-ion batteries require CC until the battery voltage reaches a predefined safety limit at which CV begins. CV charging is used in Li-ion batteries to limit the current and thus prevent the battery from overcharge. Results in Fig. 7 show CC charging [see Fig. 7(a) and (b)] and CC/CV charging [see Fig. 7(c)].

The concept of ICC was used in [12] for bulk charging with a duty cycle of $D = 0.5$ and ON time $T_{\rm on} = 3$ min. The advantage of this method in solar chargers, where the battery voltage varies during charging according to the current (or illumination) variations, is simply to let the battery rest for some time to stabilize its voltage. The drawback of this method is the long time that it takes to charge the battery if only one battery is connected to the charger.

In addition, the pulse-charging method was used in [8]. In contrary to the ICC method (see Fig. 8), where only positive pulses are injected, in pulse charging, positive and negative current pulses are injected [8]. According to [3], pulse charging offers an optimum charging, because it was developed after the chemical reactions that occur inside the battery during CC charging were studied. The main obstacle of this method is that most chargers are unidirectional, i.e., the current can flow only in one direction. To implement this method, an advanced charger with bidirectional current flow capability must be used, which might significantly increase the charger cost.

2) Temperature Control: The chemical reactions that occur inside the battery during charging produce heat. This heat increases the pressure and the temperature of the battery pack. If the battery temperature exceeds a certain value, this condition can be interpreted as a fully charged battery or a battery failure. In either case, the charger must switch to the trickle mode to protect the battery until the temperature drops to a predefined range. In [4], if a temperature rise is detected, the charger switches to the trickle charging mode until the battery is removed from the charger. This simple technique can save the battery life, at the cost of extending the charging time. In [5], the charger keeps monitoring the temperature during charging, and

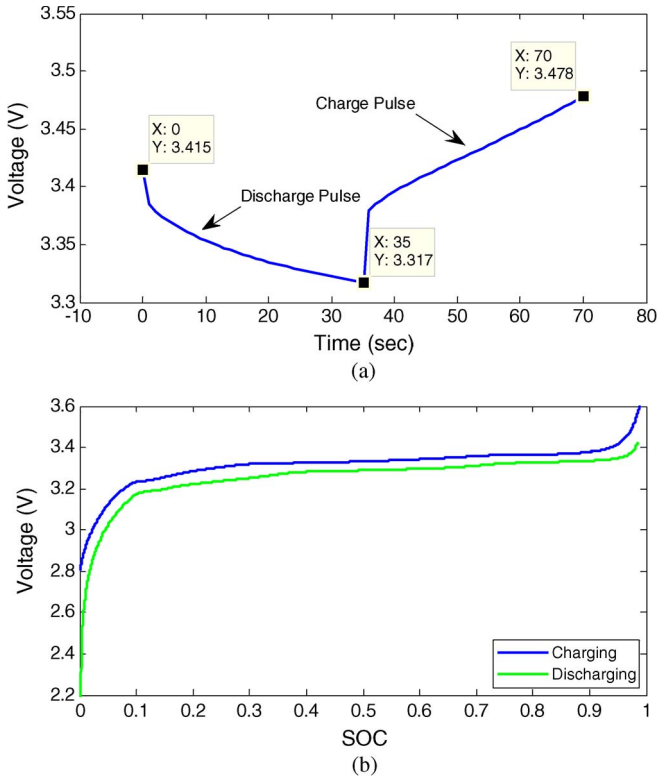

Fig. 9. Hysteresis in a Li-ion cell. (a) Hysteresis measurement test (161-mV hysteresis voltage). (b) Hysteresis for the entire SOC range.

if the temperature deviates from a predefined range, the charger will either switch from fast charging to trickle charging or show a "fault" statement until the normal temperature range resumes. The same concept was used in [8]–[10].

3) Battery-Type Identification: The identification of the battery type is exclusive for multichemistry chargers. In [13], once the OCV is measured, the algorithm allocates a possible Li-ion battery and accordingly sets a safety limit voltage. Then, the "hysteresis measurement" is performed to determine whether the battery is a nickel-based battery. According to [13], the hysteresis phenomenon was reported as a distinct feature for nickel batteries. In fact, this phenomenon was also observed in Li-ion batteries. Fig. 9 shows the hysteresis in a Li-ion cell for: 1) a 35-s 1-A discharge/charge pulse and 2) the entire SOC range. Therefore, the "hysteresis measurement" proposed in [13] is insufficient to distinguish between nickel and lithium batteries.

In [14], the charger identifies the battery chemistry slightly after the inflection point is detected. That is, if a voltage drop occurs before the voltage reaches 110% of the inflection point voltage, the battery will be either NiCd or NiMH. Otherwise, the battery is determined as Li-ion. To verify this concept, different charging tests at different currents were performed on the cells. The results showed that this concept is valid only if low currents (i.e., below $C/2$) are used. For example, the Li-ion cell was charged at C and $C/25$ rates. In the first case [see Fig. 7(c)], the inflection point was at 3.38 V, whereas in the latter case, it was 3.28 V [charging curve in Fig. 9(b)]. According to this concept, the CV mode will start when the voltage reaches 3.718 V in the first case (overvoltage) and 3.608 V (correct voltage) in the second case. With regard to the NiCd and NiMH cells, the same case was observed. At low charging rates, the peak voltage immediately before the voltage starts dropping was below 110% of the inflection point voltage, and in this case, the battery chemistry can be predicted. In practice, as the charging rates increase, the peak voltage accordingly increases due to increased internal voltage drop in the cell. In Fig. 7(a) and (b), the inflection point voltage and the peak voltage were 1.463 and 1.61 V, respectively, in both cases ($C/2$ and $3C/4$ rates were used). Based on this discussion, the inflection point concept can be applied to distinguish between nickel and lithium batteries, but to avoid overcharging a possible lithium battery, the charging rate must be low.

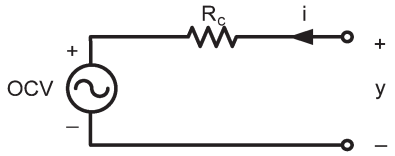

Fig. 10. Battery cell model.

4) SOC Estimation: In [5], [7]–[10], and [13], the initial SOC was predicted based on the value of the OCV. If a good estimation of the initial SOC was obtained, the performance of the charger can be improved. In practice, the accuracy of the SOC estimation from the OCV value is not guaranteed, unless the battery relaxes for a long time. Furthermore, even if the battery relaxed for a long time, its OCV will not converge to its true value (at a certain SOC) due to the hysteresis, which means that the cell voltage relaxes to a value greater than the OCV for a given SOC after charging, and relaxes to a value that is less than the OCV of that SOC after discharging. In advanced battery management systems such as electric vehicle (EV) batteries, the estimation of the SOC is substantial and must be very accurate as opposed to portable appliances, for example. If an accurate SOC estimation is required by an application, some techniques can be used, e.g., the Kalman filter, if an accurate battery model is provided. The SOC estimation through a Kalman filter can be illustrated in a simple manner. Considering a primitive cell model as shown in Fig. 10, where the charge resistance R_c and the values of OCV as a function of SOC are all provided (the values used in this example were experimentally obtained from a Li-ion cell).

If the current is assumed to be positive during charging, then the equation of the SOC z is given as

$$z(t) = z(0) + \eta \int_0^t \frac{i(\tau)}{C_n} d\tau \tag{1}$$

where $z(0)$ is the initial SOC, η is the charging or discharging efficiency, and C_n is the nominal capacity, which is defined as the number of ampere-hours obtained from a fully charged battery at a C/30 rate. In a recursive discrete-time form, the SOC is expressed as follows:

$$z_k = z_{k-1} + \left(\frac{\eta \Delta t}{C_n}\right) i_{k-1} \tag{2}$$

where k is a time index, and Δt is the time step. To estimate the SOC during charging, the extended Kalman filter (EKF) [17] is constructed as follows.

First, the model is expressed in state-space representation as

$$\begin{aligned} z_k &= f_{k-1}(z_{k-1}, i_{k-1}, \omega_{k-1}) \\ &= z_{k-1} + \left(\frac{\eta \Delta t}{C_n}\right) i_{k-1} + \omega_{k-1} \qquad (3) \\ y_k &= h_k(z_k, i_k, v_k) \\ &= OCV(z_k) + R_c i_k + v_k \\ \omega_k &\sim (0, Q_k),\ v_k \sim (0, R_k) \qquad (4) \end{aligned}$$

where $f(.)$ and $h(.)$ indicate the models' input and output equations, respectively, ω_k is an additive discrete-time white noise (process uncertainty) with a covariance matrix Q_k, and v_k is a discrete-time white noise (measurement uncertainty) with covariance matrix R_k.

Second, the filter is initialized as

$$\hat{z}_0^+ = E[z_0] \qquad (5)$$

$$P_0^+ = E\left[\left(z_0 - \hat{z}_0^+\right)\left(z_0 - \hat{z}_0^+\right)^T\right] \qquad (6)$$

where P is the estimation error covariance matrix.

Third, for $k = 1, 2, \ldots$, the following steps are performed.

1. Compute the following partial derivative matrices:

$$F_{k-1} = \left.\frac{\partial f_{k-1}}{\partial z}\right|_{\hat{z}_{k-1}^+} \qquad (7)$$

$$L_{k-1} = \left.\frac{\partial f_{k-1}}{\partial \omega}\right|_{\hat{z}_{k-1}^+}. \qquad (8)$$

2. Perform the time update of the state estimate and estimation error covariance as

$$P_k^- = F_{k-1} P_{k-1}^+ F_{k-1}^T + L_{k-1} Q_{k-1} L_{k-1}^T \qquad (9)$$

$$\hat{z}_k^- = f_{k-1}\left(\hat{z}_{k-1}^+, u_{k-1}, 0\right). \qquad (10)$$

3. Compute the following partial derivatives:

$$H_k = \left.\frac{\partial h_k}{\partial z}\right|_{\hat{z}_k^-} \qquad (11)$$

$$M_k = \left.\frac{\partial h_k}{\partial v}\right|_{\hat{z}_k^-}. \qquad (12)$$

4. Perform the measurement update as

$$K_k = P_k^- H_k^T \left(H_k P_k^- H_k^T + M_k R_k M_k^T\right)^{-1} \qquad (13)$$

$$\hat{z}_k^+ = \hat{z}_k^- + K_k\left(y_k - h_k\left(\hat{z}_k^-, 0\right)\right) \qquad (14)$$

$$P_k^+ = (I - K_k H_k) P_k^-. \qquad (15)$$

Fig. 11 shows the result of running the Kalman filter algorithm, i.e., (3)–(15), to estimate the SOC. Although the initial SOC was purposefully initialized at 0.3 instead of zero (true value), the filter converged to the true value in a relatively short time.

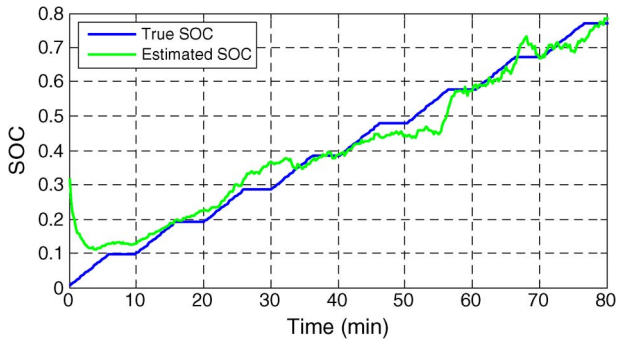

Fig. 11. SOC estimation using EKF for a Li-ion cell during the 1-A ICC charging test.

B. Termination Techniques

Different charge termination techniques were used in the discussed algorithms. These techniques are discussed and evaluated in the following discussion.

1) Voltage Drop: The voltage drop that occurs in nickel batteries, which is more obvious in NiCd, is due to the drop in the battery internal resistance when it becomes fully charged. In Fig. 7(a) and (b), the charging was terminated when a voltage drop of 30 mV occurred in the NiCd cell and 10 mV in the NiMH cell.

In NiCd and NiMH batteries, the detection of a predefined voltage drop can be used as an indication to terminate charging, as shown in [4], [6], and [12]–[14]. In [6] and [12], the concept of voltage drop was used, but with a slight modification, to overcome the voltage drops when the solar power drops. The limitation of this method in solar chargers is the random variation in the power supplied to the charger, which affects the reliability of the charger if only this technique is used. However, using this method alone is not recommended, because it will certainly overcharge the battery. Fig. 7(a) and (b) shows that the SOC was around 120% when the voltage drop was detected. This case can significantly reduce the battery lifetime.

2) Inflection Point: The concept of the inflection point is sometimes used as an indication that the battery is almost half charged. In Fig. 7(a)–(c), the inflection point occurred when the SOC approached 50%. In [4], the charger switches to trickle charging when the inflection point is detected. This method requires a very stable charging conditions such as CC and temperature to very precisely allocate the inflection point to avoid overcharging or partially charging the battery.

3) Temperature Rise: In the tests in Fig. 7, the temperature rise was 6 °C for the NiCd cell (from 24 °C to 30 °C) and 17 °C for the NiMH cell (from 25 °C to 42 °C). For the Li-ion cell, the results show almost a constant temperature during the entire range of SOC. The sudden rise in temperature, which is more obvious in NiMH cells, is a result of the undesired gases that were produced when the battery became fully charged. This unique phenomenon in NiMH batteries was employed to terminate charging (see [4] and [6]). In the temperature-based algorithm that was proposed in [6], the algorithm monitors the temperature rise of each leg and the differential temperature between the two legs. This method was proposed for solar NiMH

chargers to overcome the swing in the ambient temperature under outdoor conditions.

4) Timing: As a safety procedure, some chargers add a timer to terminate charging if a predefined timeout is reached [4], [9]. This method is very simple but can be advantageous if the charger did not detect a full charge status. However, this method cannot be used without the support of other methods.

C. Summary

A good charger must extend the battery lifetime by properly charging it. In applications where a crude SOC prediction is acceptable, e.g., in portable electronics, a simple charger with the trickle–CC–CV charging scheme is sufficient to maintain a proper operation. In outdoor environments where the ambient temperature can widely change, the charger must accommodate these variations in temperature while ensuring a proper operation. In environments where temperatures and charging rates are unexpected and can considerably change in a short time, e.g., in EVs and solar-powered chargers, more advanced techniques must be used along with the discussed charging techniques. If a dynamic SOC estimation of an application is not urgent, the variation in temperature and charging rates can be overcome by employing techniques as proposed in [6] and [12]. If a dynamic tracking of the SOC is desired in an application such as EVs, an advanced battery management system must be designed. The EV environment is extremely harsh. Temperatures can change from -30 °C to 50 °C, and different charging rates are usually used. One very effective way of overcoming these challenges is to design a battery management system with a very accurate battery model to dynamically estimate the SOC (EKF can be used, as shown earlier). If a battery model is used in the SOC estimation, it must be verified that the model is accurate enough to obtain an SOC estimation error within certain limits determined by the design specifications. In addition, the model must adapt to long-term changes in the battery characteristics (ageing effects). The battery model, regardless of how accurate it is, can be integrated with other charging algorithms to optimize the charger performance and reduce the possibility of overcharging the battery. As a summary, the capabilities of the reviewed algorithms are listed in Table I.

TABLE I
SUMMARY OF THE REVIEWED ALGORITHMS

Algorithm Reference	Supported Batteries	Charging Profile	Strengths	Limitations
4	NiCd, NiMH	CC-trickle	Different charge termination methods (very reliable)	Charge rate is not optimized
5	NiCd, NiMH	trickle-CC-trickle	Charge rate is optimized	Charge termination is based only on the cell voltage measurement
6 (Fig.2)	NiCd, NiMH	CC*-trickle	Supports solar chargers	Temperature is uncontrolled
6 (Fig.3)	NiCd, NiMH	CC*-trickle	Supports solar chargers	Battery pack must be separated into two legs
7	NiCd, NiMH	trickle-CC-trickle	Charge rate is optimized, memory effect is minimized	Temperature is uncontrolled
8	NiCd, NiMH	trickle-pulse-trickle	Charge rate is optimized, memory effect is minimized	Requires bidirectional charger for the (dis)charge pulses, support limited sizes
9	Li-Ion	CC-CV-trickle	Charge rate is optimized	Temperature is uncontrolled
10	Li-Ion	CC-CV-trickle	Cells are equalized	Charge rate is not optimized
12	NiCd, NiMH, Li-Ion	ICC-CV**	Supports solar chargers, support multiple chemistries	Unreliable for small NiMH batteries, support limited battery sizes
13	NiCd, NiMH, Li-Ion	CC-CV	Supports multiple chemistries	Battery detection is unreliable, temperature is uncontrolled
14	NiCd, NiMH, Li-Ion	CC-CV	Supports multiple chemistries	Requires very stable current and temperature, currents must be low

* Solar current is variable and is a function of illumination. However, it was considered as CC only for comparison with other algorithms.
** The CV mode in solar charges is not guaranteed because solar power is variable.

V. Trend of Recent Developments

Reliability and ease of implementation are key issues in all battery management systems, regardless of the application for which they are designed. Some recent trends of battery chargers are discussed here.

A. Reliability

Reliability in battery chargers is referred to the capability of terminating charging once a SOC of 100% is detected. This condition can be achieved through different charge termination techniques or by implementing advanced techniques, e.g., the Kalman filter, to contentiously estimate the SOC. Preventing overcharging the battery has a great impact in extending the battery lifetime and utilizing the entire battery capacity.

B. High Efficiency

The large amount of heat that is generated inside the battery during charging is an indication of a poor charging efficiency, which can reduce the battery capacity and lifetime. The charging efficiency can be increased by addressing the chemical reactions inside the battery, e.g., the pulse charging method [3]. Hence, improving charging methods according to the thermochemical behavior of the battery results in an increased efficiency, which, as a result, improves the charging speed and extends the battery lifetime.

C. Universality

As a result of the wide diversification in battery types and sizes due to the wide range of applications, a recent trend toward universal chargers has been observed [15]. Universal chargers may or may not require previous information about the battery pack prior to charging. The capability of autodetecting the battery chemistry and the number of cells with no information provided is a desired feature. This feature can be achieved by addressing the different responses of the different battery chemistries when biased to some external signals.

VI. Conclusion

Battery-charging systems have been intensively researched and developed since rechargeable batteries have been invented. However, due to the increasing demand on energy storage systems in recent applications, battery management systems have opened new doors for research and development to meet all battery system requirements. This paper has presented a review of recent charging algorithms for nickel and lithium batteries. These algorithms, which can accommodate a wide range of applications, were evaluated through some real tests on commercial battery cells. This evaluation showed the strengths and weaknesses of these algorithms, with an experimental verification, and proposed some directions for further improvement.

References

[1] Battery University Website. [Online]. Available: http://www.batteryuniversity.com
[2] Battery and Energy Technologies Website. [Online]. Available: http://www.mpoweruk.com
[3] R. C. Cope and Y. Podrazhansky, "The art of battery charging," in *Proc. 14th Battery Conf. Appl. Adv.*, 1999, pp. 233–235.
[4] J. Nicolai and L. Wuidart, "From nickel–cadmium to nickel–metal–hydride fast battery charger," STMicroelectronics Inc. Application Note. [Online]. Available: http://www.st.com/stonline/books/pdf/docs/2074.pdf
[5] T. Mundra and A. Kumar, "An innovative battery charger for safe charging of NiMH/NiCd batteries," *IEEE Trans. Consum. Electron.*, vol. 53, no. 3, pp. 1044–1052, Aug. 2007.
[6] F. Boico, B. Lehman, and K. Shujaee, "Solar battery chargers for NiMH batteries," *IEEE Trans. Power Electron.*, vol. 22, no. 5, pp. 1600–1609, Sep. 2007.
[7] M. Gonzdez, F. Ferrero, J. Antbn, and M. Pkez, "Considerations to improve the practical design of universal and full-effective NiCd/NiMH battery fast chargers," in *Proc. APEC Conf.*, 1999, pp. 167–173.
[8] J. Dıacute;az, J. Martıacute;n-Ramos, A. Pernıacute;a, F. Nuño, and F. Linera, "Intelligent and universal fast charger for NiCd and NiMH batteries in portable applications," *IEEE Trans. Ind. Electron.*, vol. 51, no. 4, pp. 857–863, Aug. 2004.
[9] Panasonic Lithium-Ion Charging Datasheet, Jan. 2007. [Online]. Available: http://www.panasonic.com/industrial/includes/pdf/Panasonic_LiIon_Charging.pdf
[10] M. Elias, K. Nor, and A. Arof, "Design of smart charger for series for lithium-ion batteries," in *Proc. PEDS Conf.*, 2005, pp. 1485–1490.
[11] M. Bhatt, W. Hurley, and W. Wölfle, "A new approach to intermittent charging of valve-regulated lead–acid batteries in standby applications," *IEEE Trans. Ind. Electron.*, vol. 52, no. 5, pp. 1337–1342, Oct. 2005.
[12] A. Hussein, M. Pepper, A. Harb, and I. Batarseh, "An efficient solar charging algorithm for different battery chemistries," in *Proc. VPPC Conf.*, Sep. 2009, pp. 188–193.
[13] H. Barth, C. Schaeper, T. Schmidla, H. Nordmann, M. Kiel, H. van der Broeck, Y. Yurdagel, C. Wieczorek, F. Hecht, and D. U. Sauer, "Development of a universal adaptive battery charger as an educational project," in *Proc. PESC*, 2008, pp. 1839–1845.
[14] S. Park, H. Miwa, B. Clark, D. Ditzler, G. Malone, N. D'souza, and J. Lai, "A universal battery-charging algorithm for Ni–Cd, Ni–MH, SLA, and Li-ion for wide-range voltage in portable applications," in *Proc. PESC*, 2008, pp. 4689–4694.
[15] F. Lima, J. Ramalho, D. Tavares, J. Duarte, C. Albuquerque, T. Marques, A. Geraldes, A. Casimiro, G. Renkema, J. Been, and W. Groeneveld, "A novel universal battery charger for NiCd, NiMH, Li-ion and Li-polymer," in *Proc. ESSCIRC Conf.*, Sep. 2003, pp. 209–212.
[16] S. Moore and P. Schneider, "A review of cell equalization methods for lithium-ion and lithium-polymer battery systems," presented at the Soc. Automotive Eng. World Congr., Detroit, MI, Mar. 2001. [Online]. Available: http://www.americansolarchallenge.org/tech/resources/SAE_2001-01-0959.pdf
[17] D. Simon, *Optimal State Estimation*, 1st ed. Hoboken, NJ: Wiley, 2006, pp. 407–409.

Ala Al-Haj Hussein (S'07) received the B.S. degree in electrical engineering in 2005 from Jordan University of Science and Technology, Irbid, Jordan, and the M.S. degree in electrical engineering in 2008 from the University of Central Florida, Orlando, where he is currently working toward the Ph.D. degree in electrical engineering with the Department of Electrical Engineering and Computer Science.

His research interests include battery management, state estimation, distributed grid-tied energy storage systems, and energy management.

Issa Batarseh (F'06) received the B.S., M.S., and Ph.D. degrees in electrical and computer engineering from the University of Illinois, Chicago, in 1983, 1985, and 1990, respectively.

From 1989 to 1990, he was a Visiting Assistant Professor with Purdue University, Calumet, IN. In 1991, he joined the Department of Electrical and Computer Engineering, University of Central Florida, Orlando, where he is currently a Professor of electrical engineering with the School of Electrical Engineering and Computer Science. He is the author or a coauthor of more than 60 refereed journal papers and 300 conference proceedings and is the holder of 14 U.S. patents. He is also the author of the textbook *Power Electronic Circuits* (New York: Wiley, 2003). His research interests include power electronics; developing high-frequency energy conversion systems to improve power density, efficiency, and performance; the analysis and design of high-frequency solar and wind energy conversion topologies; and power factor correction techniques.

Dr. Batarseh is a Registered Professional Engineer in the State of Florida and a Fellow Member of the Institution of Electrical Engineers. He served as the Chairman for the 2007 IEEE Power Electronics Specialists Conference and was the Chair of the IEEE Power Engineering Chapter and the IEEE Orlando Section.